

Towards Bayesian Data Compression

Johannes Harth-Kitzerow^{*†‡§} Reimar H. Leike[†] Philipp Arras^{†‡¶}
Torsten A. Enßlin^{†‡}

May 26, 2022

Abstract

In order to handle the large data sets omnipresent in modern science, efficient compression algorithms are necessary. There exist general purpose lossless and lossy compression algorithms, suited for different situations. Here, a Bayesian data compression (BDC) algorithm that adapts to the specific data set is derived. BDC compresses a data set under conservation of its posterior structure with minimal information loss given the prior knowledge on the signal, the quantity of interest. BDC works hand in hand with the signal reconstruction from the data. Its basic form is valid for Gaussian priors and likelihoods. This generalizes to non-linear settings with the help of Metric Gaussian Variational Inference. BDC requires the storage of effective instrument response functions for the compressed data and corresponding noise encoding the posterior covariance structure. Their memory demand counteract the compression gain. In order to improve this, sparsity of the compressed responses can be enforced by separating the data into patches and compressing them separately. The applicability of our method is demonstrated by applying it to synthetic data and radio astronomical data. Still the algorithm needs to be improved further as the computation time of the compression exceeds the time of the inference with the original data.

*jharthki@mpa-garching.mpg.de

†Max-Planck-Institut für Astrophysik, Karl-Schwarzschild-Str. 1, 85748 Garching, Germany

‡Ludwig-Maximilians-Universität München, Geschwister-Scholl-Platz 1, 80539 Munich, Germany

§Technische Universität München, James-Franck-Str. 1, 85748 Garching, Germany

¶Technische Universität München, Boltzmannstr. 3, 85748 Garching, Germany

Introduction

One of the challenges in contemporary signal processing is dealing with large data sets. Those need to be stored, processed, and analysed. They often reach the limit of the available computational power and storage. Examples include urban technology, internet searches, bio informatics and radio astronomy. In this paper we discuss, how such huge data sets can be handled efficiently by compression.

In general, data compression methods can be divided into lossless and lossy compression methods. From lossless compressed data one can regain the full uncompressed data. This limits the amount of compression archived as only redundant information can be taken away by a lossless scheme. Lossy compression is more effective in that respect, for the price of higher levels of loss of information.

In this work, the focus is on lossy compression methods. The scenario we have in mind is that of data carrying information about some variable of interest. This quantity will be called *signal* in the following. Only the relevant information for this signal needs to be conserved as much as possible. Therefore, there is no need to regain the full original data in such applications.

Many lossy compression schemes have been developed: Rate distortion theory [5, p. 301-307] gives a general approach stating the need of a loss function, which shall be minimized in order to find the best compressed representation of some original data d . As a consequence of the Karhunen-Loève theorem [11, 17, 14], principal component analysis (PCA)[18, 8] can also be used for data compression. It aims on compressing some data, such that the compressed data carries the same statistic properties as the original one. [6] showed, that PCA minimizes an upper bound of the mutual information of the original and the compressed data about some relevant signal.

Before compressing data, one should be clear about the signal on which one wants to keep as much information as possible. In a Bayesian setting, this means that the posterior probability of the signal conditional to the compressed data should be as close as possible to the original posterior that was conditioned on the original data.

The natural distance measure between original and compression posterior to be used as the action principle from which the here developed *Bayesian Data Compression* (BDC) derives, is the *Kullback Leibler* (KL) divergence [16]. Using this as the loss function reduces the problem of finding the compressed data representation to an eigenvalue problem [7]. In this work we give a didactical derivation of this and we show how this approach can be extended to nonlinear and non-Gaussian measurement situations as well as to large inference problems. This is verified using synthetic data with linear and nonlinear signal models and in a nonlinear astronomical measurement setup.

This publication is structured as follows: In sect. 1, we assume the setting of the *generalized Wiener Filter*: a linear measurement equation, for a Gaussian signal sensed under Gaussian noise. There, the optimal compression for prior mean reduces to an eigenvalue problem. In sect. 2 this is generalized to nonlinear and non-Gaussian measurements. Furthermore, we show how a sparse structure can be enforced on the compression algorithm making it possible to handle large data sets in a reasonable amount of time. In sect. 3, BDC is applied to synthetic data resulting from a linear measurement in one dimension, a nonlinear measurement in two dimensions, and real data from the Giant Metrewave Radio Telescope.

1 Linear Compression Algorithm

We approach the problem of compression from a probabilistic perspective. To this end we juxtapose the posterior probability distribution of the full inference problem with a posterior coming from a virtual likelihood together with the same prior. The goal is to derive an algorithm which takes the original likelihood and the prior as input and gives out a new, virtual likelihood that is

computationally less expensive than the original likelihood. This shall happen such that the resulting posterior probability distribution differs as little as possible from the original posterior.

The natural measure to compare the information content of a probability distribution and an approximation to it is the KL divergence [16]. Minimizing the KL divergence will lead to criteria for the most informative likelihood.

1.1 Assumptions and General Problem

The new likelihood needs to be parameterized such that the KL divergence can be minimized. Initially, we make the following assumptions:

1. The signal s , which is a priori Gaussian distributed with known covariance S , has been measured with a linear response function R_o . The resulting original data d_o is subject to additive Gaussian noise with known covariance N . In summary,

$$d_o := R_o s + n_o, \quad (1)$$

where $s \leftrightarrow \mathcal{G}(s, S)$ ($s \leftrightarrow \mathcal{G}(s - s_0, S)$ means that s is drawn from a Gaussian with mean s_0 and covariance S) and $n_o \leftrightarrow \mathcal{G}(n_o, N_o)$.

2. The compressed data d_c , which is going to be less-dimensional as compared to d_o , is related to s linearly through a measurement process with additive Gaussian noise with *unknown* covariance N_c , $d_c = R_c s + n_c$.

The posteriors of both the original and the compressed inference problem are Gaussian again [21]:

$$\mathcal{P}_i(s) := \mathcal{P}(s|d_i) = \mathcal{G}(s - m_i, D_i), \quad i \in \{o, c\} \quad (2)$$

with mean m_i and covariance D_i :

$$m_i = D_i j_i := D_i R_i^\dagger N_i^{-1} d_i \quad (3)$$

$$D_i := (S^{-1} + M_i)^{-1} \quad \text{with} \quad M_i := R_i^\dagger N_i^{-1} R_i. \quad (4)$$

Our goal is to find the *compressed measurement parameters* (d_c, R_c, N_c) such that the least amount of information on s is lost as compared to (d_o, R_o, N_o) .

This means we want to adjust d_c, R_c and N_c , such that the difference of the two posteriors of s , given the compressed data d_c and given the original data d_o , is minimal. To this end, we minimize the KL divergence under the constraint that the compressed data vector shall not exceed a certain number of dimensions:

$$\text{KL}_{o,c} := D_{\text{KL}}(\mathcal{P}_o || \mathcal{P}_c) := \int ds \mathcal{P}(s|d_o) \ln \frac{\mathcal{P}(s|d_o)}{\mathcal{P}(s|d_c)} \quad (5)$$

$$=: \langle \ln \mathcal{P}_o \rangle_{\mathcal{P}_o} - \langle \ln \mathcal{P}_c \rangle_{\mathcal{P}_o}. \quad (6)$$

A detailed derivation showing that the KL divergence is indeed the appropriate measure to decide on the optimality of the compression and a discussion about the order of its arguments can be found in [16]. For Gaussian posteriors, the KL divergence becomes

$$\text{KL}_{o,c}(d_c, R_c, N_c) = \frac{1}{2} \text{tr} \left[D_c^{-1} D_o - \mathbf{1} - \ln(D_c^{-1} D_o) + D_c^{-1} (m_c - m_o)(m_c - m_o)^\dagger \right], \quad (7)$$

where D_c and m_c depend on d_c, R_c and N_c through (3), (4). Thus, we have formulated the original compression problem as a minimization problem:

$$d_c, R_c, N_c = \operatorname{argmin}_{d_c, R_c, N_c} \operatorname{KL}_{o,c}(d_c, R_c, N_c). \quad (8)$$

In order to arrive at the optimal choice of compressed measurement parameters, we minimize $\operatorname{KL}_{o,c}$ sequentially with respect to its arguments d_c, R_c and N_c . In that procedure we keep not yet optimized parameters as given and express already optimized parameters as functions of their given parameters during their optimization. Minimization of (7) with respect to d_c for given R_c and N_c yields:

$$\begin{aligned} d_c(R_c, N_c) &= N_c (R_c D_c R_c^\dagger)^{-1} R_c m_o \\ &= (R_c S R_c^\dagger + N_c) (R_c S R_c^\dagger)^{-1} R_c m_o, \end{aligned} \quad (9)$$

using the identity

$$D R^\dagger = S R^\dagger (R S R^\dagger + N)^{-1} N. \quad (10)$$

Defining the compressed and original Wiener filter operator

$$W_i := S R_i^\dagger (R_i S R_i^\dagger + N_i)^{-1} = D_i R_i^\dagger N_i^{-1} (i \in \{c, o\}), \quad (11)$$

we see that (9) is equivalent to $R_c W_c d_c = R_c W_o d_o$ or $R_c m_c = R_c m_o$, meaning that the original and compressed posterior means are indistinguishable for the compressed response. Inserting Equation (9) back into (7), we can define the already d_c -minimized $\operatorname{KL}_{o,c}$, which only depends on the still to be optimized parameters R_c and N_c (We denote equalities up to irrelevant constants by " \cong "):

$$\begin{aligned} \operatorname{KL}_{o,c}(R_c, N_c) &:= \operatorname{KL}_{o,c}(d_c(R_c, N_c), R_c, N_c) \\ &\cong \frac{1}{2} \left(\operatorname{tr} [M_c D_o - \ln(S^{-1} + M_c)] - m_o^\dagger R_c^\dagger (R_c S R_c^\dagger)^{-1} R_c m_o \right). \end{aligned} \quad (12)$$

Only the last term of $\operatorname{KL}_{o,c}$ depends on the data. The better R_c captures m_o , the smaller this term becomes which reduces $\operatorname{KL}_{o,c}$. Thus, a response R_c that is sensitive to m_o is favoured. m_o will typically exhibit large absolute values in signal space where the original response was of largest absolute values. This gives an incentive for the compressed response towards the original one.

1.2 Information Gain from Compressed Data

The remaining task is to minimize $\operatorname{KL}_{o,c}(R_c, N_c)$ with respect to R_c and N_c . Both appear in the loss function of our choice only in the combination $M_c = R_c^\dagger N_c^{-1} R_c$ and as R_c in the last term. Let U be a unitary transformation that diagonalizes N_c . One can show that the transformation

$$R_c \rightarrow R'_c = U R_c, \quad N_c \rightarrow N'_c = U N_c U^\dagger \quad (13)$$

leaves (12) invariant:

$$\begin{aligned} m_o^\dagger R_c^\dagger (R'_c S R_c^\dagger)^{-1} R'_c m_o &= m_o^\dagger R_c^\dagger U^\dagger U (R_c S R_c^\dagger)^{-1} U^\dagger U R_c m_o \\ &= m_o^\dagger R_c^\dagger (R_c S R_c^\dagger)^{-1} R_c m_o. \end{aligned} \quad (14)$$

We use this to find a parametrization of M_c with a set of vectors $r := (r_i)_{i=1}^{k_c}$, such that

$$M_c = \sum_{i=1}^{k_c} r_i r_i^\dagger \quad (15)$$

with k_c being the number of entries of the compressed data vector d_c . In its eigenbasis N_c reads

$$N_c^{-1} = \sum_{i=1}^{k_c} \mu_i^2 e_i e_i^\dagger, \quad (16)$$

with e_i the normalized eigenvectors of N_c^{-1} and μ_i^2 the corresponding positive eigenvalues. Let us define

$$R_c := \sum_{i=1}^{k_c} e_i \hat{r}_i^\dagger, \quad \hat{r}_i := \frac{r_i}{\|r_i\|_S}, \quad \mu_i = \|r_i\|_S, \quad (17)$$

where $\|\cdot\|_S$ is the norm induced by the prior covariance ($\langle x, y \rangle_S := x^\dagger S y$, $\|x\|_S := \sqrt{\langle x, x \rangle_S}$). Then (15) holds,

$$M_c = R_c^\dagger N_c^{-1} R_c = \sum_{i,j,k=1}^{k_c} \hat{r}_i e_j^\dagger e_j e_k^\dagger e_k \hat{r}_k^\dagger \mu_j^2 = \sum_{i=1}^{k_c} r_i r_i^\dagger. \quad (18)$$

Thus, the relevant degrees of freedom of R_c and N_c are encoded in $r = (r_i)_{i=1}^{k_c}$ and we can write

$$\begin{aligned} \text{KL}_{o,c}(r) &:= \text{KL}_{o,c}(R_c(r), N_c(r)) \\ &\hat{=} \frac{1}{2} \left(\text{tr} \left[\left(\sum_i r_i r_i^\dagger \right) D_o - \ln \left(S^{-1} + \sum_i r_i r_i^\dagger \right) \right] - m_o^\dagger R_c^\dagger (R_c S R_c^\dagger)^{-1} R_c m_o \right). \end{aligned} \quad (19)$$

We are left to evaluate the trace in (12). The main issue is the logarithmic term. By decomposing $S = \sqrt{S} \sqrt{S}^\dagger$ it can be simplified:

$$\text{tr} \ln \left(S^{-1} + \sum_i r_i r_i^\dagger \right) \hat{=} \text{tr} \ln \left(\mathbb{1} + \sum_i \sqrt{S}^\dagger r_i r_i^\dagger \sqrt{S} \right). \quad (20)$$

The basis given by

$$w_i := \sqrt{S}^\dagger r_i =: \|w_i\| \hat{w}_i, \quad \forall i \in \{1, \dots, k_c\}, \quad \hat{w}_i := \frac{w_i}{\|w_i\|}, \quad (21)$$

diagonalizes both summands of (20) simultaneously:

$$\begin{aligned} \text{tr} \ln \left(\mathbb{1} + \sum_i \sqrt{S}^\dagger r_i r_i^\dagger \sqrt{S} \right) &= \text{tr} \ln \left(\mathbb{1} + \sum_i \|w_i\|^2 \hat{w}_i \hat{w}_i^\dagger \right) \\ &= \text{tr} \left[\sum_i \ln (1 + \|w_i\|^2) \hat{w}_i \hat{w}_i^\dagger \right] \\ &= \sum_i \ln (1 + w_i^\dagger w_i) \end{aligned} \quad (22)$$

In addition, the last term of (19) reduces to

$$\begin{aligned} &m_o^\dagger R_c^\dagger (R_c S R_c^\dagger)^{-1} R_c m_o \\ &= m_o^\dagger \sum_i \hat{r}_i e_i^\dagger \left(\sum_{j,k} e_j r_j^\dagger S r_k e_k^\dagger \right)^{-1} \sum_l e_l \hat{r}_l^\dagger m_o \\ &= m_o^\dagger \sum_{i,l} \hat{r}_i e_i^\dagger e_l \hat{r}_l^\dagger m_o = m_o^\dagger \sum_i \hat{r}_i \hat{r}_i^\dagger m_o, \end{aligned} \quad (23)$$

such that we get

$$\begin{aligned} \text{KL}_{\text{o,c}}(r) &\hat{=} \frac{1}{2} \left(\text{tr}[S^{-1}m_{\text{o}}m_{\text{o}}^{\dagger}] + \sum_{i=1}^{k_c} [r_i^{\dagger}D_{\text{o}}r_i - \ln(1 + r_i^{\dagger}Sr_i) - m_{\text{o}}^{\dagger}\hat{r}_i\hat{r}_i^{\dagger}m_{\text{o}}] \right) \\ &\hat{=} - \sum_{i=1}^{k_c} \Delta I(w_i), \end{aligned} \quad (24)$$

with

$$2\Delta I(w_i) := -w_i^{\dagger}\mathcal{D}_{\text{o}}w_i + \ln(1 + w_i^{\dagger}w_i) + \hat{w}_i^{\dagger}\tilde{m}_{\text{o}}\tilde{m}_{\text{o}}^{\dagger}\hat{w}_i, \quad (25)$$

$$\mathcal{D}_{\text{o}} := \sqrt{S}^{-1}D_{\text{o}}\sqrt{S}^{-\dagger}, \quad \tilde{m}_{\text{o}} := \sqrt{S}^{-1}m_{\text{o}}, \quad \sqrt{S}^{-\dagger} := \sqrt{S}^{\dagger-1}. \quad (26)$$

We see that the relevant part of $\text{KL}_{\text{o,c}}$ splits up into a sum over independent contributions $-\Delta I(w_i)$ associated to the individual vectors w_i , each of which belongs to a specific compressed data point $(d_c)_i$. Since $\text{KL}_{\text{o,c}}$ expressed this way is additive with respect to the inclusion of additional data points, the sum in (24) can easily be extended. To optimize $\text{KL}_{\text{o,c}}$ with respect to w (or r respectively), the contributions $\Delta I(w_i)$ can be minimized individually with respect to their respective eigenvectors w_i .

The information gain ΔI depends on the normalized eigendirection \hat{w}_n and its magnitude $\|w_n\|$,

$$2\Delta I(\hat{w}_n, \|w_n\|) := -\|w_n\|^2\hat{w}_n^{\dagger}\mathcal{D}_{\text{o}}\hat{w}_n + \ln(1 + \|w_n\|^2) + \hat{w}_n^{\dagger}\tilde{m}_{\text{o}}\tilde{m}_{\text{o}}^{\dagger}\hat{w}_n. \quad (27)$$

We maximize this with respect to the norm

$$\|w_n\|^2 = \frac{1}{\hat{w}_n^{\dagger}\mathcal{D}_{\text{o}}\hat{w}_n} - 1, \quad (28)$$

and insert the result into (27). This leaves us with our final expression of the information gain of a single compressed data point:

$$\boxed{2\Delta I(\hat{w}_n) = \hat{w}_n^{\dagger}\mathcal{D}_{\text{o}}\hat{w}_n - 1 - \ln(\hat{w}_n^{\dagger}\mathcal{D}_{\text{o}}\hat{w}_n) + \hat{w}_n^{\dagger}\tilde{m}_{\text{o}}\tilde{m}_{\text{o}}^{\dagger}\hat{w}_n.} \quad (29)$$

Summarizing, with $\{e_i\}$ and $\{r_i\}$ we found representations of the compressed noise covariance and compressed measurement response, such that the trace in $\text{KL}_{\text{o,c}}$ splits up into independent summands. Each summand is the negative information gain, when adding another dimension for the compressed data vector. An additional compressed data point should maximize this information gain. These maximizations can be performed one after the other. As a next step we need to maximize $\Delta I(\hat{w}_n)$.

1.3 Optimal Expected Information Gain

In order to find the compressed data point which adds most information to the compressed likelihood, (29) needs to be minimized with respect to \hat{w}_n . For zero posterior mean $m_{\text{o}} = 0$, this problem reduces to an eigenvalue problem as shown in Appendix 5. We proceed by treating the general case of non-vanishing m_{o} .

There is only one normalized vector \hat{w}_i (respectively \hat{r}_i) left to be determined for each $i \in \{1, \dots, k_c\}$. However, in the current form, (29) cannot be maximized analytically. The main issue is the last term, that contains \tilde{m}_{o} and which we treat stochastically using the prior signal and noise knowledge on the signal s and the noise n_{o} only. Thereby, we can calculate the expected information gain.

Using the Gaussian priors of signal s and noise n_o with zero mean, as well as the measurement (1) and the definition (3) of m_o , we get the expected posterior signal mean

$$\langle m_o \rangle_{\mathcal{P}(s, n_o)} = D_o R_o^\dagger N_o^{-1} (R_o \underbrace{\langle s \rangle_{\mathcal{P}(s)}}_{=0} + \underbrace{\langle n_o \rangle_{\mathcal{P}(n_o)}}_{=0}) = 0, \quad (30)$$

and variance

$$\begin{aligned} C &:= \langle m_o m_o^\dagger \rangle_{\mathcal{P}(s, n_o)} = D_o R_o^\dagger N_o^{-1} (R_o S R_o^\dagger + N_o) N_o^{-1} R_o D_o \\ &= (D_o R_o^\dagger N_o^{-1} (R_o S R_o^\dagger + N_o) N_o^{-1} R_o + \mathbb{1}) D_o - D_o \\ &\stackrel{(10)}{=} (S R_o^\dagger N_o^{-1} R_o + \mathbb{1}) D_o - D_o \\ &\stackrel{(4)}{=} S - D_o. \end{aligned} \quad (31)$$

Thus, as a sum of Gaussian distributed variables, m_o again is Gaussian distributed with

$$\mathcal{P}(m_o) = \mathcal{G}(m_o, C). \quad (32)$$

Calculating the mean of (29) under this distribution then gives

$$\boxed{\langle \Delta I(\hat{w}_n) \rangle_{\mathcal{P}(m_o)} = -\frac{1}{2} \ln(\hat{w}_n^\dagger \mathcal{D}_o \hat{w}_n)}. \quad (33)$$

This expected information gain is maximal, if and only if \hat{w}_n is parallel to the eigenvector of \mathcal{D}_o with smallest eigenvalue δ_n^2 . This insight reduces the problem to the eigenvalue problem

$$\mathcal{D}_o w_n = \delta_n^2 w_n. \quad (34)$$

In terms of r , which builds M_c in (15), and after inserting (4) this states

$$D_o^{-1} S r_n = (\mathbb{1} + M_o S) r_n = \delta_n^{-2} r_n. \quad (35)$$

(17) and (28) are then equivalent to

$$\boxed{M_o S r_n = \mu_n^2 r_n}. \quad (36)$$

For $r_n = R_o^\dagger v$, this is equivalent to the generalized eigenvalue problem of [7],

$$R_o S R_o^\dagger v = \lambda N_o v, \quad (37)$$

multiplied with $R_o^\dagger N_o^{-1}$ from the left.

The expected information gain for including the compressed data point d_{cn} therefore is

$$\begin{aligned} \Delta I(\mu_n) &:= \langle \Delta I(\hat{r}_n) \rangle_{\mathcal{P}(m_o)} = -\frac{1}{2} \ln(\hat{w}_n \underbrace{\mathcal{D}_o \hat{w}_n}_{=\delta_n^2 \hat{w}_n}) \\ &= -\ln(\delta_n) = \frac{1}{2} \ln(\mu_n^2 + 1). \end{aligned} \quad (38)$$

Let us discuss why the eigenvalue problem (35) specifies the most informative compressed representation of the original data. Multiplying (35) by $r_n^\dagger D_o$ from the left, we get

$$r_n^\dagger S r_n = \delta_n^{-2} r_n^\dagger D_o r_n. \quad (39)$$

Let us recall that at the most informative directions r_n , the signal inference with original data updates our prior knowledge the most. There, $r_n D_o r_n$, the posterior uncertainty with respect to the direction r_n , is much smaller than $r_n^\dagger S r_n$, the corresponding prior uncertainty. This implies via Equation (39), that for those δ_n^{-2} will be large. And just those are the eigendirections favoured by ΔI via Equation (38).

Summarizing, we need to find the k_c largest eigenvalues μ_n^2 and corresponding vectors r_n of (36). With these, the compressed measurement parameters are

$$N_c^{-1} = \sum_{n=1}^{k_c} \mu_n^2 e_n e_n^\dagger, \quad (40)$$

$$R_c = \sum_{n=1}^{k_c} e_n \hat{r}_n^\dagger, \quad (41)$$

$$d_c = (R_c S R_c^\dagger + N_c) (R_c S R_c^\dagger)^{-1} R_c m_o, \quad (42)$$

with

$$\hat{r}_n := \frac{r_n}{\|r_n\|_S} \quad \text{and} \quad \|r_n\|_S = \mu_n. \quad (43)$$

These equations and (3) and (4) are all ingredients needed to solve the compression problem.

1.4 Algorithm

Now, the previously derived method shall be turned into the actual BDC. For that we first estimate the fraction of information stored in the compressed measurement parameters computing only a part of all eigenpairs $(\mu_n^2, r_n)_n$ determining those. Then, we discuss some details of how to compute the input parameters for getting the compressed measurement parameters, i. e. for the eigenvalue problem (36) and how to solve it.

Due to computational limits, in general we cannot determine all K eigenpairs of (36) carrying information. We need to set the number k_{\max} of most informative eigenpairs being determined numerically. For those, we derive a lower bound of the information stored in the compressed measurement parameters in the following. If we are only interested in a certain amount of information we can use this bound to find and neglect eigenpairs containing too little information, such that in the end, we have $k_c \leq k_{\max}$ eigenpairs containing still enough information.

The eigenpairs carrying information are those with non-zero eigenvalue μ_i . The number K of non-zero eigenvectors is equal to the rank of $M_o S$. As Gaussian covariances, S and N_o are positive definite and therefore have full rank. R_o has at most a rank equal to the smaller rank of both covariances. Thus, with (4), the rank of $M_o S$ and therefore K is equal to the rank of R_o .

First, we find an upper bound for the total information $I := \sum_{i=1}^K \Delta I(\mu_i)$ of all K eigenpairs. The eigenpairs are ordered such that the eigenvalues decrease with growing index, and therefore the contribution to the total information sum I . Hence, we can give an upper limit bound to the amount of information lost by truncating the sum at k_c , and adding the number of eigenvalues ignored, $K - k_{\max}$, times the largest amount of information provided by any of the unknown distributions, $I(\mu_{k_{\max}})$. Thus,

$$I \leq \sum_{i=1}^{k_{\max}} \Delta I(\mu_i) + (K - k_{\max}) \Delta I(\mu_{k_{\max}}), \quad (44)$$

For the fraction γ of information contained in the eigenpairs compared to the total information I it follows:

$$\begin{aligned}\gamma &:= \frac{\sum_{i=1}^{k_c} \Delta I(\mu_i)}{I} \\ &\stackrel{(44)}{\geq} \frac{\sum_{i=1}^{k_c} \Delta I(\mu_i)}{\sum_{i=1}^{k_{\max}} \Delta I(\mu_i) + (K - k_{\max}) \Delta I(\mu_{k_{\max}})} \\ &=: \gamma_{\min} \left(k_c, (\mu_i)_{i=1}^{k_{\max}}, K \right).\end{aligned}\tag{45}$$

Using $I \geq \sum_{i=1}^{k_{\max}} \Delta I(\mu_i)$, we analogously find an upper limit

$$\gamma \leq \gamma_{\max} := \frac{\sum_{i=1}^{k_c} \Delta I(\mu_i)}{\sum_{i=1}^{k_{\max}} \Delta I(\mu_i)}\tag{46}$$

for γ , which we can use to narrow it.

Now we can find the minimum number of eigenpairs containing at least $\gamma_{\min} I$ information by finding the smallest k_c such that (45) holds and then forget all eigenpairs with a larger index than k_c . Then we know $\gamma \in [\gamma_{\min}, \gamma_{\max}]$.

In case $k_{\max} > K$, some eigenpairs contain no additional information to the prior knowledge and

$\Delta I(\mu_{k_{\max}}) = 0$. Then we have stored all information ($\gamma = 1$) in the compressed data with non-zero eigenvalue and Equation (45) is automatically fulfilled.

When evaluating (3) we have to avoid the inversion of S or \sqrt{S} as the explicit inversion of a $n \times n$ matrix is of $\mathcal{O}(n^3)$. Such expensive operations can be partly avoided by getting m_o via

$$\begin{aligned}m_o &= \sqrt{S} \tilde{m}_o = \sqrt{S} \mathcal{D}_o \tilde{j}_o \\ &= \sqrt{S} (\mathbf{1} + \sqrt{S}^\dagger R_o^\dagger N_o^{-1} R_o \sqrt{S})^{-1} \sqrt{S}^\dagger R_o^\dagger N_o^{-1} d_o.\end{aligned}\tag{47}$$

Compared to directly calculating m_o with Equations (3) and (4), this saves one inversion of S^{-1} . Still the linear operator $(\mathbf{1} + \sqrt{S}^\dagger R_o^\dagger N_o^{-1} R_o \sqrt{S})$ needs to be inverted. In this case we can make use of the conjugate gradient algorithm which computes the application of the inverse of a matrix to a vector in $\mathcal{O}(n)$.

The eigenvalue problem (36) can then be solved by an Arnoldi iteration [15].

This leaves us with basic BDC as summarized in Algorithm 1.

In the linear scenario the full Wiener filter needs to be solved. Thus, the computational resources required to compute and store the compressed measurement parameters exceed the resources saved by the compression. It would be of benefit in a real world application if the eigenfunctions could be re-used in repetitions of the same measurement. BDC's main benefit lies in the nonlinear scenario, when the inference appears to be more complicated, but BDC enables to exploit information stored in data further while calling the original data and response less often.

2 Generalizations

2.1 Generalization to Nonlinear Case

The derivation of BDC so far is based on a linear measurement equation. In real world problems, however, often nonlinear measurement equations

$$d = R(s) + n\tag{48}$$

Algorithm 1 Basic Bayesian Data Compression

- 1: **procedure** COMPRESS(\sqrt{S} , R_o , N_o^{-1} , d_o , k_{\max} , γ)
 - 2: $m_o = \sqrt{S}(\mathbf{1} + \sqrt{S}^\dagger R_o^\dagger N_o^{-1} R_o \sqrt{S})^{-1} \sqrt{S}^\dagger R_o^\dagger N_o^{-1} d_o$
 - 3: $S = \sqrt{S} \sqrt{S}^\dagger$
 - 4: compute largest eigenpairs $(\mu_i^2, r_i)_{i=1}^{k_{\max}}$ of $R_o^\dagger N_o^{-1} R_o S$
 - 5: find smallest k_c , such that (45) holds.
 - 6: **for** every $i > k_c$ **do**
 - 7: forget (μ_i^2, r_i)
 - 8: **for** every $i \leq k_c$ **do**
 - 9: $r_i \leftarrow \frac{r_i}{\sqrt{r_i^\dagger S r_i}}$
 - 10: $R_c = \sum_{i=1}^{k_c} e_i r_i^\dagger$, with unit vectors $\{e_i\}_{i=1}^{k_c}$
 - 11: $N_c^{-1} = \text{diag}((\mu_i^2)_{i=1}^{k_c})$
 - 12: $d_c = (R_c S R_c^\dagger + N_c)(R_c S R_c^\dagger)^{-1} R_c m_o$
 - 13: **return** d_c, R_c, N_c^{-1}
-

describe the relation of signal and data. There, the response transforms the signal nonlinearly. In addition, the signal parameters can be very non-Gaussian and inter-dependent through a deep hierarchical model. In those cases we need to adjust Basic BDC.

Let us assume, that such complications are expressed via a deep hierarchical model. Following [12], deep hierarchical models can be transformed into independent standard normal distributed parameters by encoding prior knowledge into the likelihood. In this fashion the complexity of a deep hierarchical model is stored in a nonlinear function f . That relates the parameters s of the hierarchical model – the actual signal – to the parameters ξ of a transformed, flattened, non-hierarchical model via

$$s = f(\xi). \quad (49)$$

The transformation f has to be chosen such that the prior of ξ becomes a standard normal distribution:

$$\mathcal{P}(d|s)\mathcal{P}(s)ds = \mathcal{P}(d|f(\xi))\mathcal{G}(\xi, \mathbf{1})d\xi. \quad (50)$$

For flattened models we can now deal with nonlinear measurement setups using Metric Gaussian Variational Inference (MGVI) [13]. There, the posterior is approximated by a Gaussian $\mathcal{G}(\xi - \bar{\xi}, \Xi)$ with inverse Fisher information metric as uncertainty covariance Ξ centered on some mean value $\bar{\xi}$. The Fisher information metric is

$$M_{d|s} = \left\langle \frac{\partial \mathcal{H}(d|s)}{\partial s^\dagger} \frac{\partial \mathcal{H}(d|s)}{\partial s} \right\rangle_{P(d|s)}. \quad (51)$$

Here

$$\mathcal{H}(d|s) := -\ln \mathcal{P}(d|s) \quad (52)$$

is the information Hamiltonian of the likelihood. With a standard Gaussian prior, the posterior covariance then states

$$\Xi^{-1} = J_\xi^\dagger M_{d|s} J_\xi + \mathbf{1} \quad \text{with} \quad J_\xi := \frac{\partial f(\xi)}{\partial \xi}. \quad (53)$$

For many measurement situations, the response splits into a linear part R_{lin} and a nonlinear part R_{nl}

$$d_{\text{o}} = R_{\text{lin}}R_{\text{nl}}(s) + n_{\text{o}}. \quad (54)$$

(The linear part might describe a linear telescope response, or just be an identity operator.) Then we redefine our signal $s' := R_{\text{nl}}(s)$. Before, s were the parameters of the hierarchical model with a function f transforming standard Gaussian distributed ξ into s . Now s' are our parameters being related to ξ via $R_{\text{nl}} \circ f$. Thus, the Jacobian states

$$J'_{\xi} = \frac{\partial R_{\text{nl}}(f(\xi))}{\partial \xi} \quad (55)$$

and we define

$$\sqrt{S'} := \left. \frac{\partial R_{\text{nl}}(f(\xi))}{\partial \xi} \right|_{\xi=\bar{\xi}}. \quad (56)$$

This is a linearization of the nonlinear part evaluated at $\bar{\xi}$, a reference value of ξ , *e.g.* the current mean location provided by the MGVI algorithm, such that

$$J'_{\bar{\xi}}{}^{\dagger} M_{d|\bar{\xi}} J'_{\bar{\xi}} = \sqrt{S'}^{\dagger} M_{d|\bar{\xi}} \sqrt{S'}. \quad (57)$$

The compression is then applied to the linear measurement equation

$$d_{\text{o}} = R_{\text{lin}}s' + n_{\text{o}} \quad (58)$$

with given noise covariance N_{o} . This way, we have all the ingredients for BDC to work in the nonlinear case as well.

During the inference process, the approximated mean $\bar{\xi}$, at which the linearization is evaluated, changes. With updated knowledge also the compression input will change. This suggests the following strategy:

1. Compress the original measurement parameters with prior knowledge and original measurement parameters as input.
2. Infer the posterior mean given the compressed measurement parameters. This will only be an approximate solution.
3. Approximate the original posterior around the inferred mean and use it as the new prior to start again with the first step.

We will call the number of compressions, *i.e.* the number of total repetitions of those three steps, n_{comp} , the number of MGVI minimization steps to infer the mean with compressed data in between n_{rep} . In total the original data and response only have to be used n_{comp} times, while in total we reach $n_{\text{comp}} \times n_{\text{rep}}$ minimization steps exploiting the information in the data. A crucial step will be to find the optimal exploration (n_{comp}) versus exploitation (n_{rep}) ratio as in [20].

2.2 Enforcing sparsity

High dimensional data are difficult to handle simultaneously. For the eigenvalue problem of BDC, it is more efficient to solve a larger number of less dimensional problems. For the signal inference, it is beneficial to ensure that the response R_{c} and noise N_{c} of the compressed system are sparse

operators. This can be achieved by dividing the data into patches to be compressed separately. This also has the advantage of less dimensional eigenvalue problems to be solved, saving computation time. The separately compressed data of the patches as well as corresponding responses and noise covariances are finally concatenated. Alternatively this method can be used to compress data online, i. e. while data is measured one can collect and process it blockwise as suggested by [4], such that the full data never has to be stored completely.

Mathematically speaking, we divide the original data d_o into separated sets of data d_{o_i} with responses R_{o_i} and noise covariance N_{o_i} for every patch i . Then we compress those data sets separately leading to d_{c_i} , R_{c_i} and N_{c_i} . Concatenating them back again leads to the final measurement equation

$$\underbrace{\begin{pmatrix} d_{c1} \\ \vdots \\ d_{cn} \end{pmatrix}}_{d_c} = \underbrace{\begin{pmatrix} R_{c1} \\ \vdots \\ R_{cn} \end{pmatrix}}_{R_c} s + \underbrace{\begin{pmatrix} n_{c1} \\ \vdots \\ n_{cn} \end{pmatrix}}_{n_c} \quad (59)$$

with noise covariance

$$N_c = \begin{pmatrix} N_{c1} & & \\ & \ddots & \\ & & N_{cn} \end{pmatrix}. \quad (60)$$

In the following we will call this process *patchwise compression*. If the compression of all original data is done at once, we call it *jointly compression*. With patchwise compression, noise correlations between data points of different patches get lost. Signal correlations, however are still represented via the signal correlation S , and therefore also present in the compressed signal posterior.

To summarize, we ideally separate the data into noise-uncorrelated patches. The data of every patch is compressed separately leading to compressed measurement parameters for every patch. By concatenating those, we get all operators needed for the compressed signal posterior. This removes the need to store the compressed responses over the entire signal domains. Only their patch values have to be stored, saving memory and computation time.

3 Application

Now, the performance of BDC is discussed for applications of increasing complexity. First a linear synthetic measurement setting, then a nonlinear one. For the latter, we demonstrate the advantage of dividing the data into patches and compressing them separately. Finally, the compression of radio interferometric data from the Giant Metrewave Radio Telescope (GMRT) is discussed.

3.1 Synthetic Data: Linear Case

First, the BDC is applied to synthetic data in the Wiener filter context. The signal domain is a one dimensional regular grid with 256 pixels. The synthetic signal and corresponding synthetic data are drawn from a zero centered Gaussian prior. The data is masked, such that only pixels 35 to 45 and 60 to 90 are measured linearly, according to $d = Rs + n$. Additionally white Gaussian noise is added with zero mean and standard deviation of $\sigma_n = 0.2 \cdot 10^{-2}$ for measurements up to pixel 79, and $0.4 \cdot 10^{-2}$ for pixels 80 to 90. Those noisy data are then compressed to four data points, from which the signal is inferred in a last step.

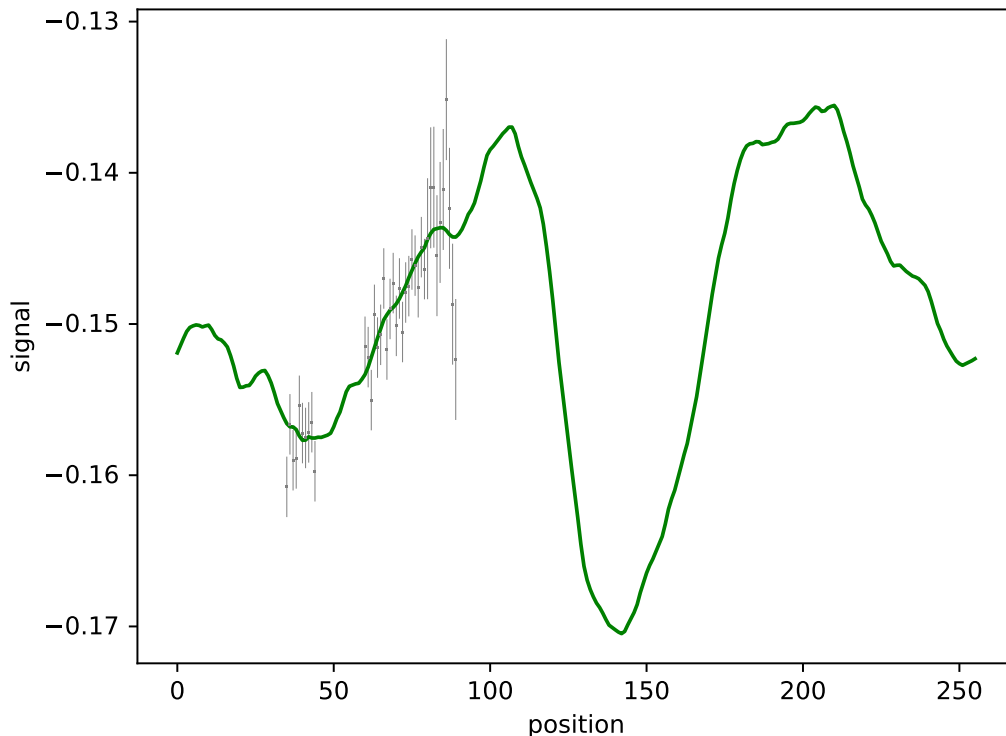


Figure 1: One dimensional synthetic data setup to test BDC. The synthetic signal is marked in green and the measured data in gray.

The signal covariance is assumed to be diagonal in Fourier space, with the power spectrum

$$P_s(k) := \frac{2 \cdot 10^4}{1 + \left(\frac{k}{20}\right)^4}. \quad (61)$$

The signal itself can be computed from the power spectrum via

$$s = \mathbb{F} \sqrt{P_s(k)} \xi_k \quad (62)$$

with a Fourier or Hartley transformation \mathbb{F} and the Fourier modes ξ_k being drawn independently from a standard Gaussian $\mathcal{G}(\xi, 1)$. The response is set to be a mask measuring pixels 35 to 45 and 60 to 90 directly, with a local and thereby unity response. The measurement setup with signal mean, synthetic signal, and data are shown in Figure 1.

We apply Basic BDC. For the eigenvalue problem we use the python wrapper of the Arnoldi method “eigs” from the `scipy.sparse.linalg` library [9].

After having compressed the data, we evaluate the reconstruction performance using the compressed data. With Equation (2) the posterior can be calculated directly from the compressed measurement parameters, and signal covariance. The posterior mean and uncertainty for the original and the compressed data are compared to the ground truth in Figure 2. The original data

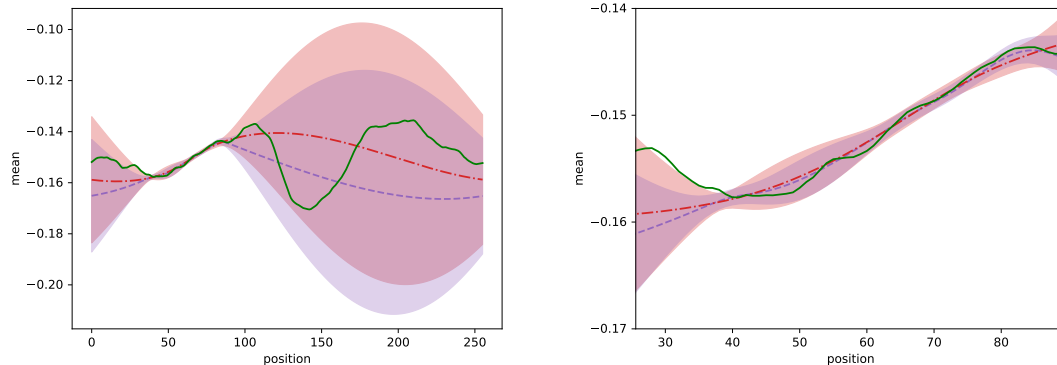


Figure 2: Inference of synthetic signal (green) in a linear Wiener Filter setup. The posterior mean given the original data shown in Figure 1 is plotted as dashed purple line with shades marking its standard deviation. The same for the posterior mean given four compressed data points as dash-dotted red lines with corresponding shades. The left graph shows the full domain, the right one a zoom in the measured area.

has been compressed from 40 to 4 data points. Especially at the location of the data, both the original and the compressed reconstruction are close to the ground truth.

Figures 2 and 3 show that the compression posterior has a higher variance than the original data posterior. Since the compression method is lossy, i.e. information is lost in the process of compression, a higher variance of the compression posterior is reasonable. Especially in the measured area, the uncertainty of the compression posterior is a bit higher.

The eigenvectors are plotted in Figure 3. At the masked pixels, the eigenvectors stay zero. The changing noise covariance visibly impacts the shape of the eigenvectors. Between pixels 79 and 80, where the noise increases, is a clear break in all the eigenvectors. A higher noise standard deviation leads to abrupt drops in the eigenvectors. A more detailed discussion of the eigenvectors can be found in Appendix 6. An analytical derivation of their form in the simple setting of a continuous mask and constant noise is given in Appendix 7.

We found that the compression method reduces the dimension of the data with minimal loss of information in the simple case of a linear 1D Wiener Filter inference. Storing only four compressed data points still reproduces the signal well. Every compressed data point determines the amplitude of an eigenvector such that the signal is approximated appropriately. The lossy compression leads to a slightly higher uncertainty, as information is lost.

3.2 Synthetic Data: Nonlinear Case

Now BDC should be tested on data from a nonlinear generated signal in two dimensions. This should verify the derivation of the nonlinear approximation in Section 2.1 and also test the idea of patchwise compression from Section 2.2. Some nonlinear synthetic signal is generated and then inferred with the original data, with compressed data, and with data, which has been first divided into patches and then compressed. The results are discussed with respect to the quality of the inferred mean for the different methods, their standard deviation, their power spectrum, as well as the computation time.

The synthetic signal has been generated with a power spectrum created by a nonlinear amplitude model as described in [2] deformed by a sigmoid function. (The signal and data generat-

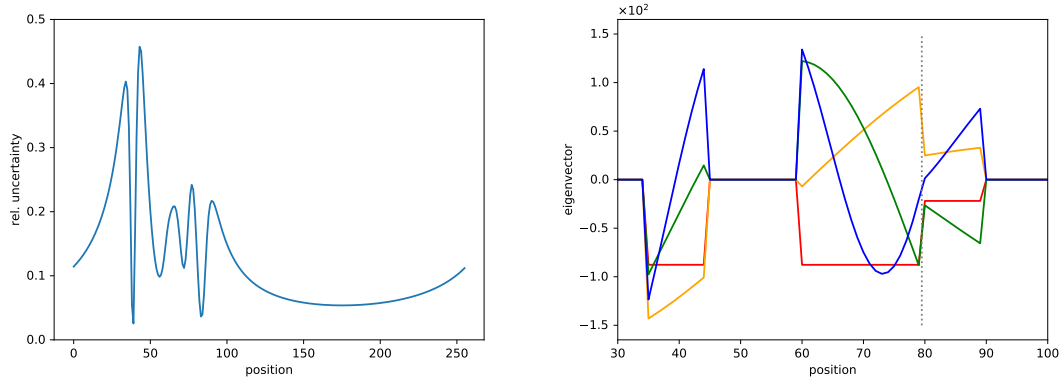


Figure 3: To the left the relative uncertainty excess of the compressed reconstruction with respect to the one based on the original data. To the right the relevant part of the eigenvectors of the eigenvalue problem (36) for the synthetic data setup in Figure 1 over the signal domain. The eigenvectors are colored in red, orange, green, and blue in descending order of their eigenvalues. The gray dotted line marks the noise level change.

ing functions can be found here: <https://gitlab.mpcdf.mpg.de/jharthki/bdc>.) The resulting ground truth lies on an 128 times 128 regular grid and is shown on the top left most panel of Figure 4. This signal is covered by a four by four checkerboard mask with equally sized 32 times 32 squares, as displayed in the second top panel of Figure 4. Additionally noise with zero mean and 0.02 standard deviation has been added. From this incomplete and noisy data, the non-Gaussian signal as well as the power spectrum of the underlying Gaussian process need to be inferred simultaneously. The results of the original inference are plotted in the third top panel of Figure 4.

After setting up the input parameters for BDC, the data was compressed from 8192 to $k_{\max} = 80$ data points altogether without sorting out less informative data points. Next Metric Gaussian Variational Inference [13] performed $n_{\text{rep}} = 2$ inference steps based on the compressed data, each time finding a better approximation for the posterior mean and approximating the posterior distribution again. Then the original data was compressed again using the current posterior mean as the reference point ξ . This was done $n_{\text{comp}} = 3$ times in total. To determine the amount of information contained in the resulting compressed data another run has been started where 4096 eigenpairs have been computed. This way the estimation of γ using Equations (46) and (45) is more exact. With this we estimate that the compressed data of size 80 contains 31.4% to 32.2% of the information. The same way, one gets that 672 compressed data points contain 80% of the information. It turns out that already 80 compressed data points contain enough information to reconstruct the essential structures of the signal. The corresponding posterior mean is plotted in the center left of Figure 4 together with the difference to the originally inferred mean. Overall the compression yields similar results. Deviations appear at the edges of homogeneous structures. The variance is plotted in the center right of Figure 4. Again it differs mainly at the edges. Since during the compression process information is lost, the results should have higher uncertainty in general. This is almost everywhere the case, however, there are some parts, which report a better significance than the reconstruction without compression. This either implies an inaccuracy of BDC or that BDC can partly compensate the approximation MGVI brings into the inference by

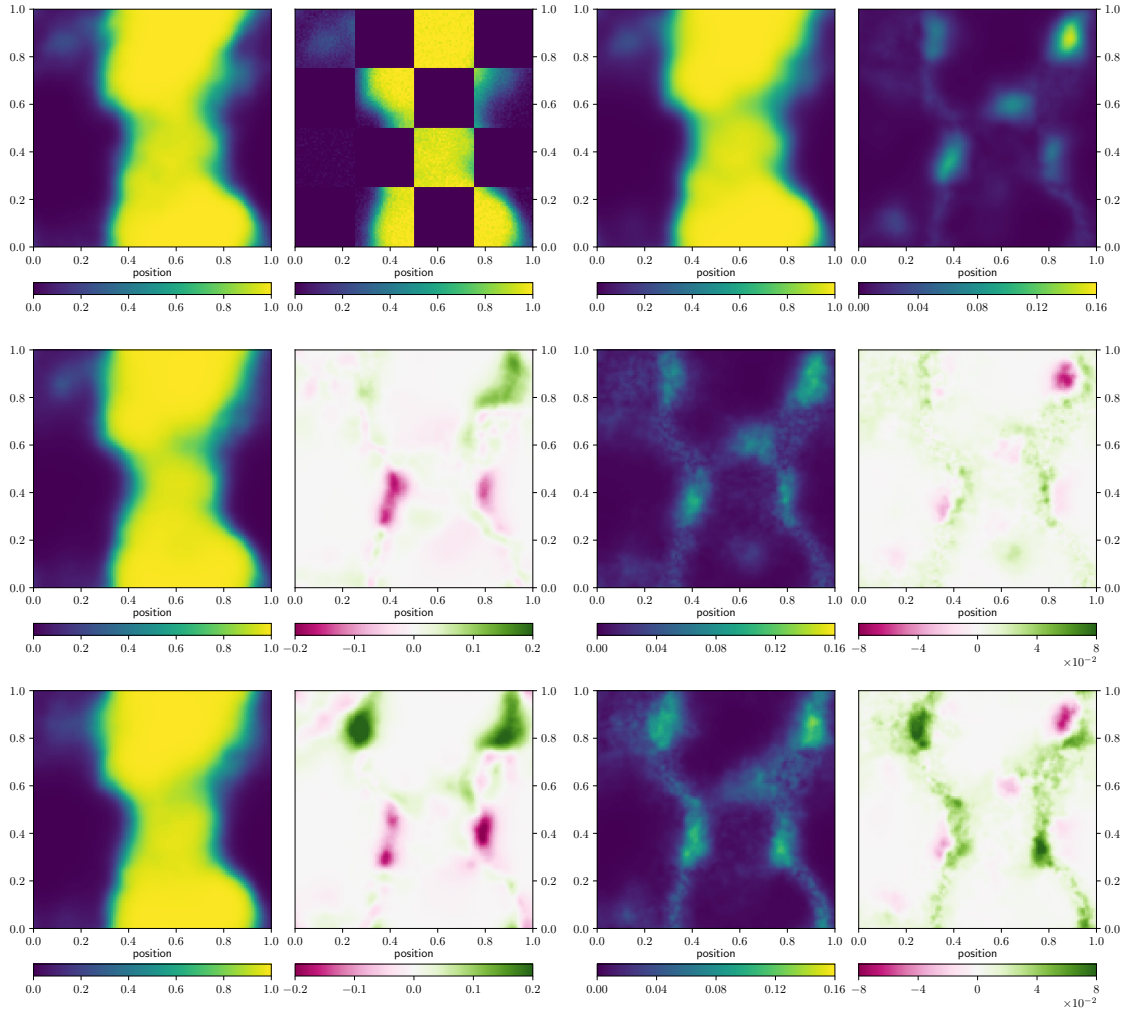


Figure 4: *Top row:* From left to right: First, the generated ground truth and second, the synthetic data for a synthetic signal created by the amplitude model and processed by a sigmoid function. A unity response connects the data and the signal with a four times four checkerboard mask hiding the signal from the data. Third, using MGVI, the posterior mean of the signal and fourth, its uncertainty as inferred with the original data. *Middle row:* Results for compressing the data globally (not patchwise). Three compression and MGVI steps were performed. First, the posterior mean. Second, its difference to the mean of the inference without compression, i.e. the compression mean subtracted from the original mean. Third, the posterior variance of the inference with compressed data. And fourth, the same, subtracted from the variance of the posterior with the original data. *Bottom row:* As in the middle, just with patchwise compressed data.

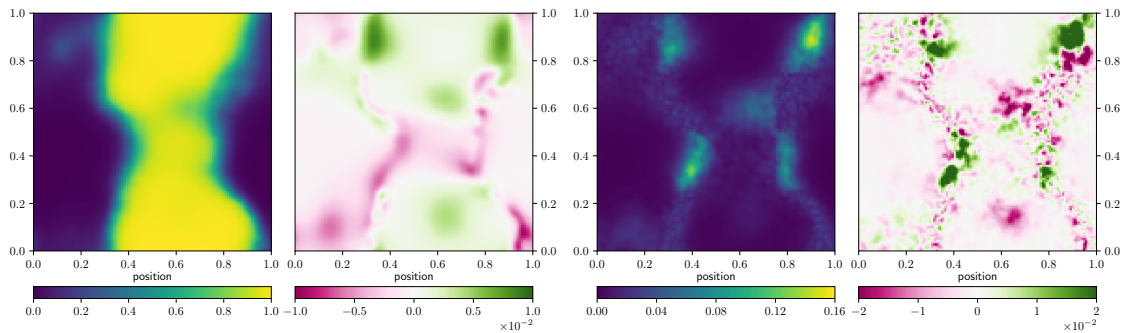


Figure 5: Mean (left) and Variance (right) computed from the compressed measurement parameters according to Equation (4) and its difference to the same computed by MGVI as in Figure 4.

providing it with measurement parameters that are better formatted for its operation.

Now we investigate patchwise compression in the same setup. The data in each of the eight measured squares were compressed to $k_{\max} = 10$ data points separately. In total there are as many compressed data points for the patchwise compression as for the jointly one. We can use that the response only masks the signal but does not transform it. Thus, we can compress the data with prior information of the corresponding patch only. This way we reduce the dimension of the eigenvalue problem (36) to the size of the patch. The resulting mean and variance of the inference for this method and their difference to the original ones are shown in the lower part of Figure 4. Both differ mainly at the edges of homogeneous structures from the original posterior mean and variance. Also for the case of patchwise compressed data, the variance at some points becomes smaller than for the original inference. Like in the case of compressed data, we improve the estimation of γ by computing 4096 eigenpairs, i.e. 512 eigenpairs per patch. It turns out that for every patch 15.9% to 16.7% of information is kept when using the 10 most informative eigenpairs for the compressed data points. When comparing the γ values of each patch one needs to consider that the patches are compressed individually. Therefore the information of one and another patch might be partly redundant and their individual γ s can not just be added in order to get the joint information content.

After having computed the compressed measurement parameters, we can also directly get the compression posterior mean and covariance from Equations (3) and (4). The inference from the compressed data then reduces to a linear Wiener Filter problem. The resulting mean and variance are plotted in Figure 5. This illustrates that the compression helped to linearize the inference problem around the posterior mean.

Finally the results of the methods can be compared by looking at the inferred power spectra in Figure 6. All of the reconstructions recover the power spectrum qualitatively. It stands out that the samples of the original inferred power spectrum tend to lie below the ground truth, while the reconstructions of the two compression methods are rather a bit higher.

It is interesting to have a closer look on the back projection of the compressed data, i.e. $R_c^\dagger d_c$ as well as on the projection of the eigenvectors building the compressed responses onto the space. The back projection of the jointly compressed data before the first inference, i.e. having looked at the original data only once, is shown in Figure 7 on the left. In contrast to the back projection after the minimization process in the right plot, the data look quite uninformative, covering more or less uniformly the whole probed signal domain. After the inference, the reference point changes around which the linearization is made, the jointly compressed data addresses mainly regions of rapid changes in the signal. Especially the contours at the edges are saved in the jointly compressed

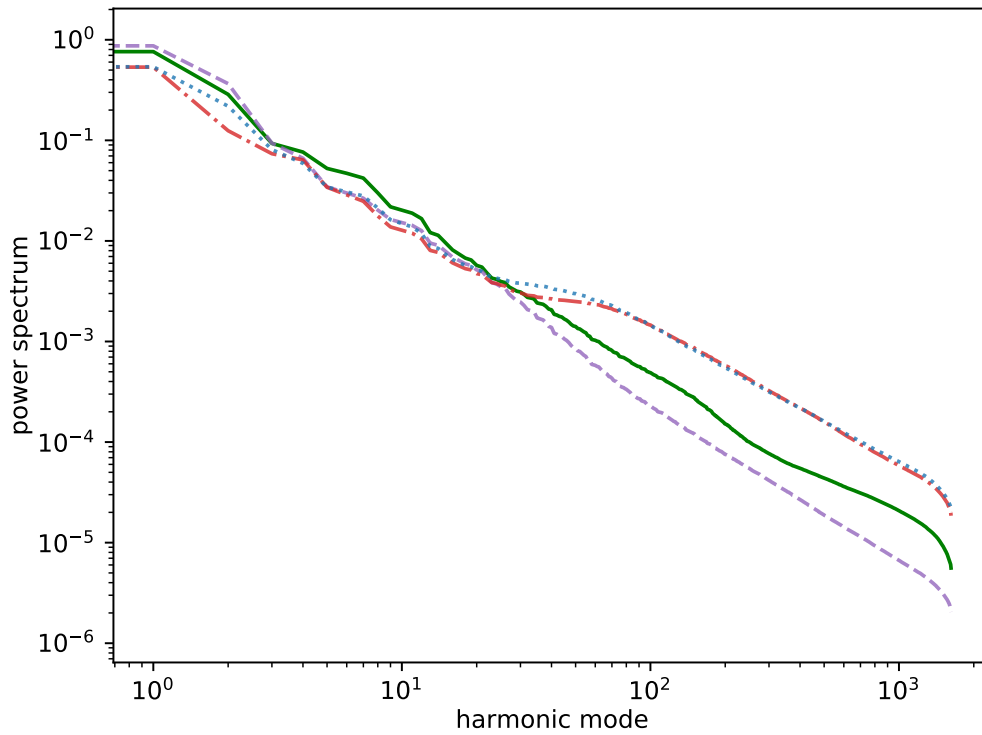


Figure 6: The power spectrum of the ground truth (solid, green) and the inference using the different methods: The mean (dashed, purple) of power spectra for different samples drawn from the original data posterior is plotted with shades marking their standard deviation. The power spectra for jointly compressed data (dash dotted, red) and with patchwise compressed data (dotted, blue) are plotted the same way.

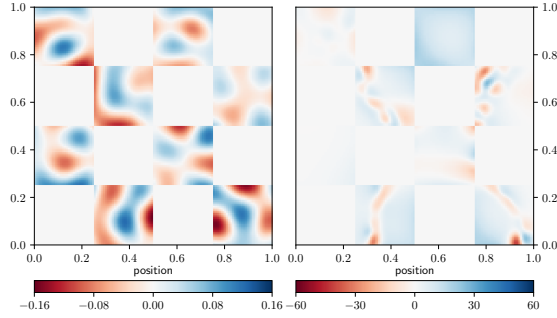


Figure 7: The back projected jointly compressed data before (left) and after (right) the inference.

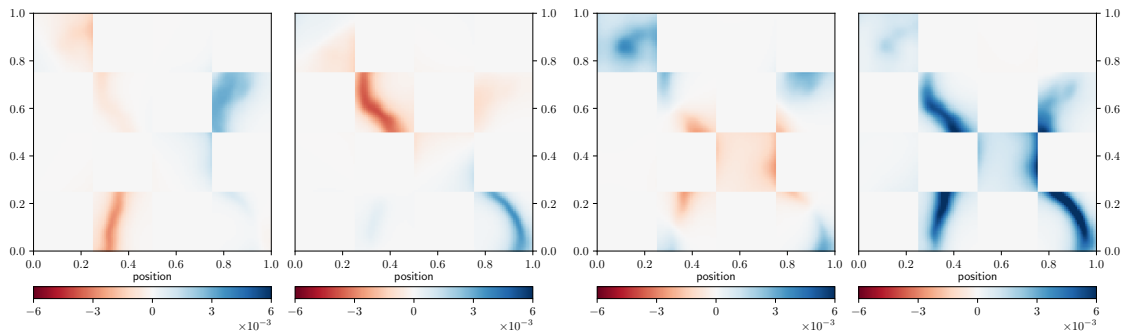


Figure 8: The eigenvectors, i.e. the row vectors of the jointly compressed data response after the inference corresponding to the highest eigenvalues in descending order from left to right.

data. This is even clearer visible in the projection of the eigenvectors r_i building the compressed response according to (17) in Figure 8. The first two eigenvectors capture the frame of the big structure. The third one mainly looks at the upper left corner, where also some structure occurs, though it is less distinct than the big one. None of the eigenvectors covers any structure in the upper slightly right patch. Since the structure of the ground truth there is rather uniform, it does not contain much information but the amplitude of the field.

Figure 9 shows the back projection of the patchwise compressed data before and after the inference. Here, the change of the basis functions becomes apparent as well.

Table 1 shows the computation time of the different compression methods and reconstructions. As described above, it has been measured for $(n_{\text{rep}}, n_{\text{comp}}) = (2, 3)$, as well as $(n_{\text{rep}}, n_{\text{comp}}) = (3, 2)$. In case of the original inference in total $n_{\text{rep}} \times n_{\text{comp}}$ inference steps were performed such that in there are an identical number of inference steps for every method. The time has been measured for the inference only and for the total run of separation of the data into patches, n_{comp} compressions with n_{rep} inferences after each compression. The average of all $n_{\text{rep}} \times n_{\text{comp}}$ inferences is given in the first line of table 1. The time for the total runs is given in the second line. It has been measured on a single node of the FREYA computation facility of the Max Planck Computing & Data Facility restricted to 42 GB RAM, with 2 x Intel(R) Xeon(R) Gold 6138 CPU @ 2.00GHz and 40 cores. In all categories the inference with patchwise compressed data is the fastest.

In addition the number of response calls were counted for $(n_{\text{rep}}, n_{\text{comp}}) = (2, 3)$. In case the original response is expensive, it is favourable to call it as few as possible. In the inference with the

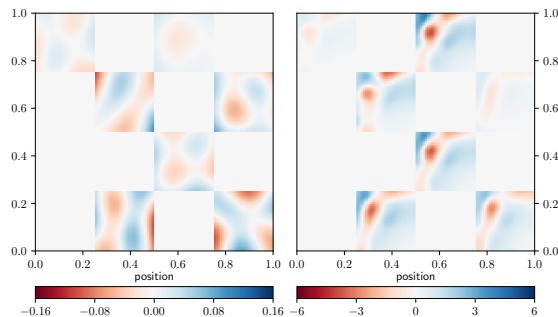


Figure 9: Back projection of the patchwise compressed data before (left) and after (right) the inference.

original data, R_o was called 686 187 times, in the process of compressing jointly it was called 4 369 times. During the patchwise compression, the patchwise original response has been called 14 102 times. In the case of patchwise compression the response only maps between the single patches, i. e. it is a factor 16 smaller than the full response. Thus, effectively the full original response has been called only about 881 times in the case of patchwise compression leading to a speed up factor of up to 780 in case the response calculation is the dominant term.

3.3 Real data: Radio interferometry

Finally, we apply BDC to radio astronomical data from the supernova remnant Cassiopeia A observed by the GMRT [1, 19]. 200 000 data points from the measurement were selected randomly and noise corrected according to [3]. Using those, two images were constructed by the RESOLVE algorithm [10, 3] that rests on MGVI one with and, for comparison, one without compression.

In the following, the model used by RESOLVE as described in [10] is adopted. To this end, the variables from the amplitude model in [10] are denoted as ξ and transformed to the sky s – the actual signal – by $s = f(\xi)$ as described in [12]. The data are connected to the sky s via a nonlinear measurement equation of the form (54). The nonlinear part of the response R_{nl} contains a pointwise exponentiation and a Fourier transformation onto a grid, which leads to the variable of interest for the compression method s' . The linear part of the response R_{lin} degrid the resulting points and transforms them to the data d_o , i. e. it projects the points lying on a grid to continuous space. The total response $R = R_{lin} \circ R_{nl}$ directly maps from the sky s to the data d_o , such that we have the measurement equations

$$d_o = R(s) + n \quad (63)$$

$$= R_{lin}(R_{nl}(s)) + n \quad (64)$$

$$= R_{lin}(s') + n. \quad (65)$$

R_{lin} is computationally expensive and the data d_o are large. The aim is to compress those with the signal s' as the variable of interest. It turns out that the jointly compression of all data is not possible due to its large computational costs. So only the patchwise compression is tested. Similar to the previous example, a non-Gaussian signal and the power spectrum of the underlying Gaussian process need to be estimated simultaneously from noisy and very incomplete data, only here the nonlinearity is an exponential function and the sparse data live in Fourier space.

We divide the Fourier plane into 64 times 64 squared patches, as shown in Figure 10. The location of the measurements in the Fourier plane are marked as well. It is apparent that many

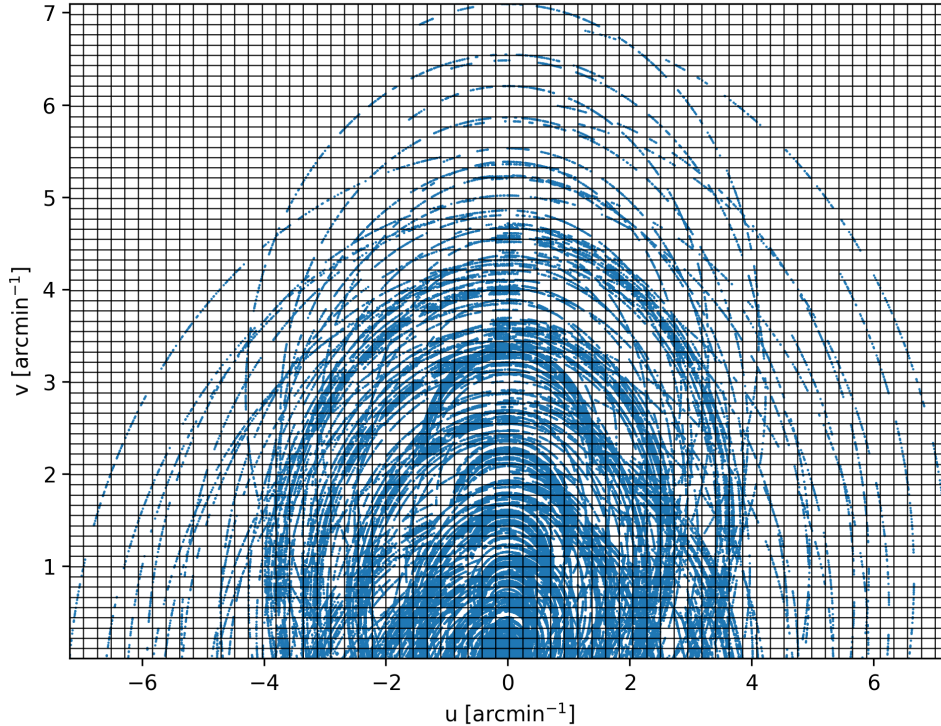


Figure 10: The position of all data points in Fourier space. The overlaid grid marks the data patches according to a Cartesian grid.

patches are free of data, some contain some data, and the highest density of data points occurs around the origin of the Fourier plane.

Figure 11 shows the image obtained from the original dataset and from the patchwise compressed dataset. The mean is obtained after three MGVI iteration steps from the original data. Using BDC, the data in each patch was compressed ideally under prior information.

The resulting data, noise covariance and responses were concatenated and used for inference in MGVI with three inference steps. The received posterior distribution was used to compress the separated original data once more with updated knowledge, inferred with three minimization steps. Doing this one more time resulted in the reconstruction shown here. The bottom right plot in Figure 11 shows that the uncertainty variance of the reconstruction from patchwise compressed data is mostly higher than the variance from the original reconstruction. This is expected due to the information loss of the compression. The data points in every patch have been compressed to maximally 64 data points. The fraction γ has been set to 0.99. In total this led to 73 239 compressed data points, which is a reduction of the data size by a factor 2.73. Due to the large computation time it is not possible to determine more eigenpairs. Thus, estimates of the amount of information γ contained in the compressed data points are very vast. In average, the estimated range of γ is 0.35% to 94.8% for every patch with a standard deviation of 0.39% and 17.3% respectively. The dispersion of those values for different patches is high, caused by the varying

distribution of data points per patch.

The corresponding power spectra are shown in Figure 12. They only partly agree within their standard deviations but roughly in their slope.

This shows that BDC is able to operate on real world data sets in the framework of radioastronomical image reconstruction. The run time still can be improved, though. Since the compression for different patches works independently, this can perfectly be parallelized. Another potential area for improvement would be the choice of the separation of the patches. Two criteria need to be considered therefor: From a computational perspective patches with few data points are favoured. From information theoretical point data points carrying similar information shall be compressed together. Besides Euclidian gridded patches, we also performed a separation of the data in equiradial and equiangular patches. This lead to a more even distribution of data points inside the patches, since this way patches become larger further outside, where there are less data points. However, for this patch pattern small structures in the reconstruction got lost. The reason for that is that data points in the Fourier plane far away from the origin store information about the small scale image structures. Compressing them together therefore can be expected to lead to a loss of information on small structures.

4 Conclusion

A generic Bayesian data compression algorithm has been derived, which compresses data in an optimal way in the sense that as much information as possible about the signal is stored given prior knowledge on the signal. Our derivation is based on the Kullback-Leiber divergence. It reproduces the results of [7] that optimizing the information loss function leads to a generalized eigenvalue problem. We generalized the method to the nonlinear case with the help of Metric Gaussian Variational Inference [13]. Also, we divided the data set into patches to limit the computational resources needed for the compression. This enforces sparseness of the response, allowing to apply the method in high dimensional settings as well.

The method has been successfully applied to synthetic and real data problems. In an illustrative one dimensional synthetic linear scenario, 256 data points could be compressed to four data points with almost no loss of information. In a more complex, two dimensional and nonlinear synthetic measurement scenario, 8192 measurements could be reduced to 80 data points with a reasonable loss of information. Dividing the data into patches resulted in a huge reduction of the required computation time for the compression itself, confirming the expected advantage.

Finally, the method has been applied to real astrophysical data. The radio image of a supernova remnant has been reconstructed qualitatively with a data reduction by a factor of almost 3.

Still, the current BDC algorithm requires too much resources in terms of storage needed for the responses and computation time. In order to improve this even further, the choice of the data patches can still be investigated and informationally optimized such that data points storing similar information are thrown in the same patch. Up to now, data have been patched which are neighbouring in real or Fourier space. However also data points could be informationally connected non-locally. One would need to look at the Kullback-Leibler divergence again to find those connections and group the data accordingly.

Another problem is the computational cost of the response. In the course of our derivation we represented it in a vector decomposition. One could demand further restrictions to those vectors such as a certain parametrization or find other representations to find an computationally ideal basis for the responses.

As a final step BDC needs to prove its advantage in real applications. A promising application could be online compression such as [4] suggest. In a scenario, where data come in blockwise, those

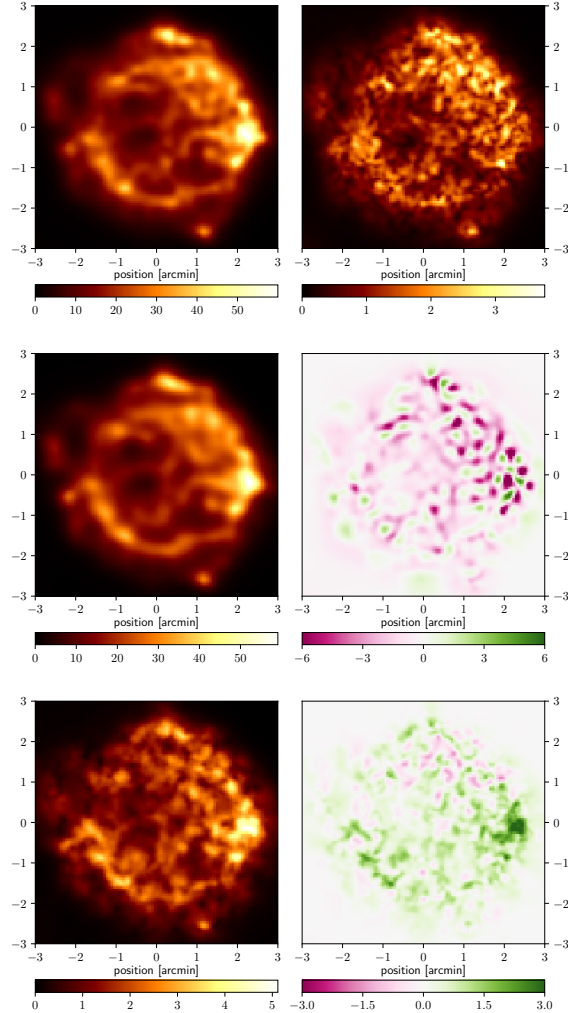


Figure 11: The reconstruction of supernova remnant Cassiopeia A from GMRT measurements. The colorbars have units Jy arcmin^{-2} . *Top row:* To the left the resulting posterior mean, to the right its variance using original data. *Middle row:* To the left reconstructed mean using patchwise compressed data. To the right its difference to the reconstructed mean from original data. *Bottom row:* The same for the posterior variance.

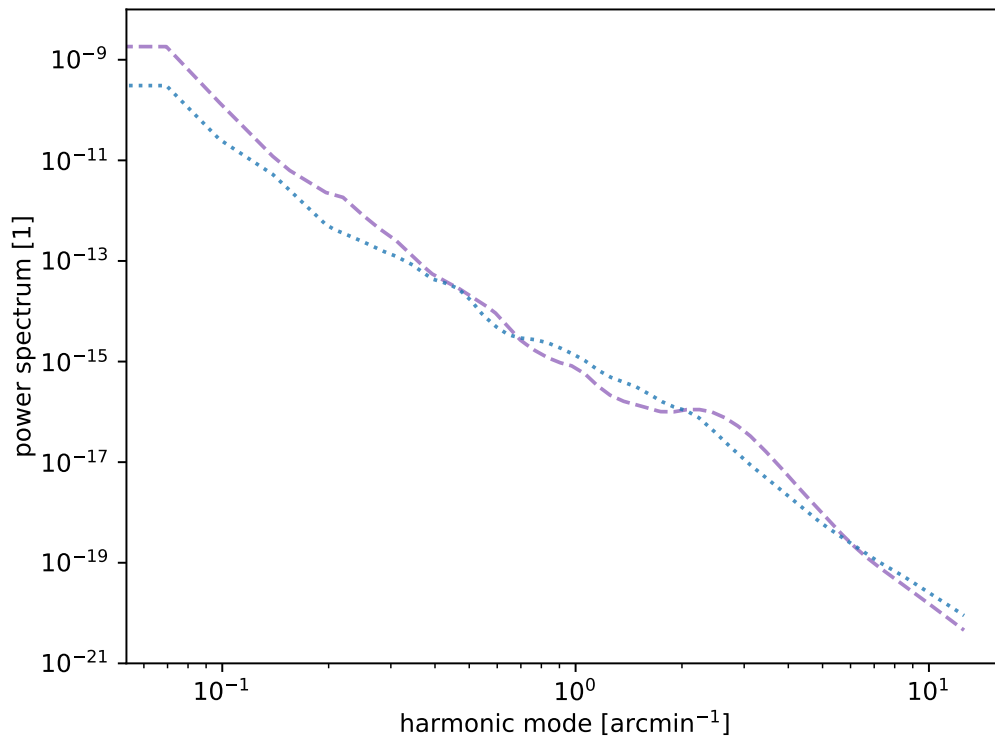


Figure 12: Such as in Figure 6, the mean of power spectra for different samples drawn from the original data posterior (dashed, purple) and the patchwise compressed data posterior (dotted, blue) with shades marking their standard deviation.

blocks can be treated as the patches and compressed separately. This is for example applicable in any experiment running over time. There, time periods imply the measurement blocks. This way the original data never needs to be stored at all, but compressed immediately and optimally under the current knowledge.

Acknowledgements

J. Harth-Kitzerow acknowledges financial support by the Deutsche Forschungsgemeinschaft (DFG, German Research Foundation) under Germany's Excellence Strategy – EXC-2094 – 390783311.

P. Arras acknowledges financial support by the German Federal Ministry of Education and Research (BMBF) under grant 05A17PB1 (Verbundprojekt D-MeerKAT).

References

- [1] S. Ananthkrishnan. The Giant Meterwave Radio Telescope / GMRT. *Journal of Astrophysics and Astronomy Supplement*, 16:427, 1995.
- [2] P. Arras, P. Frank, R. Leike, R. Westermann, and T. A. Enßlin. Unified radio interferometric calibration and imaging with joint uncertainty quantification. *A&A*, 627:A134, 2019.
- [3] P. Arras, R. A. Perley, H. L. Bester, R. Leike, O. Smirnov, R. Westermann, and T. A. Enßlin. (Preprint) *arXiv:2008.11435*, v1, submitted: Aug 2020.
- [4] X. Cai, L. Pratley, and J. McEwen. Online radio interferometric imaging: Assimilating and discarding visibilities on arrival. *Monthly Notices of the Royal Astronomical Society*, 485, 12 2017.
- [5] T. M. Cover and J. A. Thomas. *Elements of information theory*. Wiley-Interscience publication, Hoboken, NJ, 2nd edition, 2006.
- [6] B. C. Geiger and G. Kubin. (Preprint) *arXiv:1205.6935*, v2, submitted: Jan 2013.
- [7] L. Giraldi, O. P. Le Maître, I. Hoteit, and O. M. Knio. Optimal projection of observations in a Bayesian setting. *Computational Statistics & Data Analysis*, 124:252 – 276, 2018.
- [8] I. T. Jolliffe. *Principal component analysis*. Springer series in statistics. Springer, New York i.a., 2010.
- [9] E. Jones, T. Oliphant, P. Peterson, et al. SciPy: Open source scientific tools for Python, 2001. accessed Oct 2020.
- [10] H. Junklewitz, M. R. Bell, M. Selig, and T. A. Enßlin. Resolve: A new algorithm for aperture synthesis imaging of extended emission in radio astronomy. *A&A*, 586:A76, 2016.
- [11] K. Karhunen. *Über lineare Methoden in der Wahrscheinlichkeitsrechnung*. Annales Academiae Scientiarum Fennicae: Ser. A 1. Sana, 1947.
- [12] J. Knollmüller and T. A. Enßlin. (Preprint) *arXiv:1812.04403*, v1, submitted: Dec 2013.
- [13] J. Knollmüller and T. A. Enßlin. (Preprint) *arXiv:1901.11033*, v3, submitted: Jan 2020.
- [14] D. D. Kosambi. Statistics in function space. *Journal of the Indian Mathematical Society*, 7:76–88, 1943.

Table 1: Computation times for the inference with original, compressed, and patchwise compressed data in the nonlinear synthetic application. Also the number of original response calls is stated. The original data has been inferred $n_{\text{rep}} \times n_{\text{comp}}$ times.

$(n_{\text{rep}}, n_{\text{comp}}) = (3, 2)$	original	comp	patchcomp
Inference time [sec]	317	1040	285
Total run time [sec]	634	2085	579
No. response calls	686187	2913	6850
$(n_{\text{rep}}, n_{\text{comp}}) = (2, 3)$			
Inference time [sec]	208	716	196
Total run time [sec]	623	2154	604
No. response calls	686187	4369	14102

- [15] R. Lehoucq, D. Sorensen, and C. Yang. *ARPACK Users' Guide*. Software, environments, tools. Society for Industrial and Applied Mathematics, Philadelphia, 1998.
- [16] R. Leike and T. Enßlin. Optimal Belief Approximation. *Entropy*, 19(8):402, 2017.
- [17] M. Loève. Fonctions aleatoires du second ordre. *Processus stochastique et mouvement Brownien*, page 366, 1948.
- [18] K. Pearson. Liii. on lines and planes of closest fit to systems of points in space. *The London, Edinburgh, and Dublin Philosophical Magazine and Journal of Science*, 2(11):559–572, 1901.
- [19] W. Raja. *Faraday Slicing Polarized Radio Sources*. PhD thesis, Jawaharlal Nehru University New Delhi, 09 2014.
- [20] M. Vergassola, E. Villermaux, and B. I. Shraiman. ‘infotaxis’ as a strategy for searching without gradients. *Nature*, 445(7126):406–409, 2007.
- [21] N. Wiener. *Extrapolation, interpolation and smoothing of stationary time series*. Technology Press of the Mass. Inst. of Technology [u.a.], Cambridge, Mass. [u.a.], 1949.

5 Optimality of BDC for Zero Posterior Mean

In this paragraph we prove that for $m_o = 0$ the compression is optimal, if \hat{w}_i is the eigenvector to the smallest eigenvalue of \mathcal{D}_o . Optimal means that $2\Delta I(\hat{w}_i)$ in (29) is maximal with respect to \hat{w}_i .

Proof: For the proof, the \hat{w}_i dependence in (29) needs to be shown explicitly:

$$2\Delta I(\hat{w}_i) := \hat{w}_i^\dagger \mathcal{D}_o \hat{w}_i - 1 - \ln(\hat{w}_i \mathcal{D}_o \hat{w}_i) \quad (66)$$

Let $\{(v_i, \delta_i)\}$ be the eigenpairs of \mathcal{D}_o . The eigenvectors $\{v_i\}_i$ form a complete orthonormal basis. Then \hat{w}_i can be written as $\hat{w}_i = \sum_j \omega_{ij} v_j$ with $\sum_j \omega_{ij}^2 = 1$, such that \hat{w}_i is normalized, and

$$\begin{aligned} 2\Delta I(\hat{w}_i) &= 2\Delta I\left(\sum_j \omega_{ij} v_j\right) \\ &= \sum_j \omega_{ij}^2 \delta_j - 1 - \ln\left(\sum_j \omega_{ij}^2 \delta_j\right). \end{aligned} \quad (67)$$

We will use that $f(x) = x - 1 - \ln x$ is a convex function. This can be easily verified by calculating the first derivative

$$\partial_x f(x) = 1 - \frac{1}{x} \quad (68)$$

and the second one

$$\partial_x^2 f(x) = \frac{1}{x^2} > 0. \quad (69)$$

We observe that $2\Delta I(\hat{w}_i) = f(\sum_j \omega_{ij}^2 \delta_j)$. By Jensen's inequality we get

$$\begin{aligned} 2f\left(\sum_j \omega_{ij}^2 \delta_j\right) &\leq \sum_j \omega_{ij}^2 2f(\delta_j) \\ &\leq \sum_j \omega_{ij}^2 2f(\min_k(\delta_k)) \\ &= 2f(\min_k(\delta_k)) \underbrace{\sum_j \omega_{ij}^2}_{=1}. \end{aligned} \quad (70)$$

Note, we used here that $f(x)$ has its minimum at $x = 1$ and that the eigenvalues of \mathcal{D}_o are between 0 and 1, i.e. the smaller eigenvalues maximize $f(\delta_i)$. This way we got an upper bound reached for $\omega_i = \delta_{0i}$, where v_0 is the eigenvector corresponding to the smallest eigenvalue $\delta_0 := \min_k(\delta_k)$. \square

Doing data compression by just considering the smallest eigenvalues of D_o will be found to be the right choice when considering $\langle \Delta \text{KL}_{o,c}(\hat{r}_i) \rangle_{P(m_o)}$ as a loss function in the section 6. This gives the expected loss for the expected mean of $m_o = 0$ under $\mathcal{P}(m_o) = \mathcal{P}(m_o|S, R_o, N_o)$.

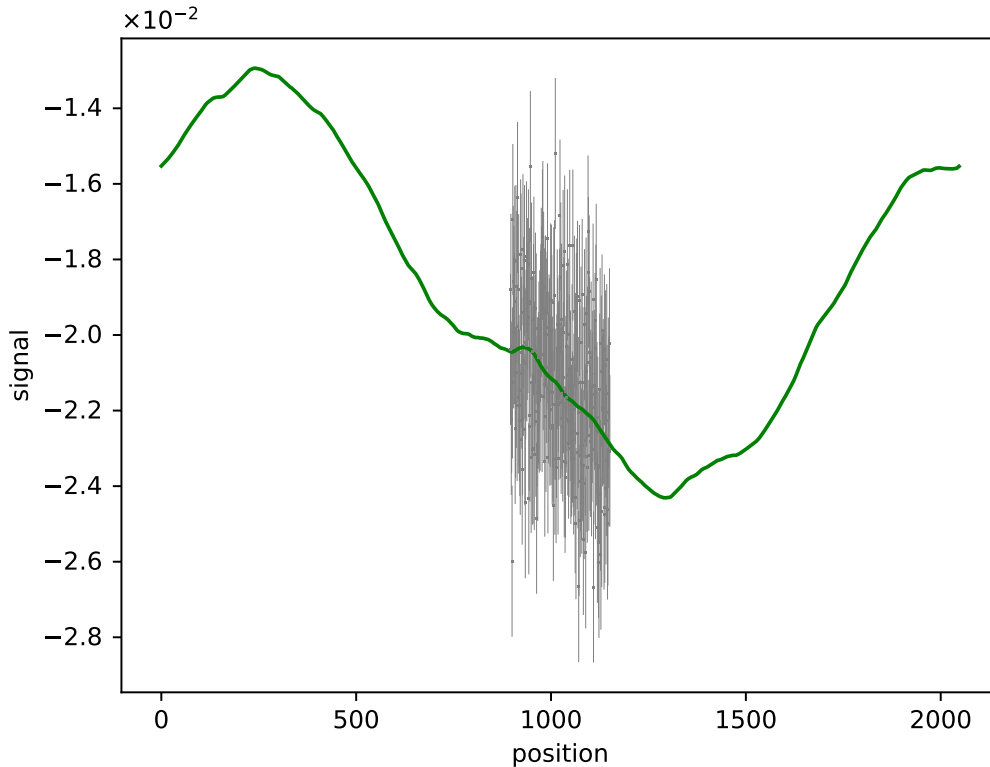


Figure 13: One dimensional synthetic data setup to test BDC. The synthetic signal is marked in green and the measured data in gray.

6 1D Wiener Filter Data Compression

In Section 3.1 we applied our data compression method to synthetic data in the context of the generalized Wiener Filter with a linear measurement equation. In this section, we are going to investigate the shape of the eigenfunctions corresponding to the eigenproblem of (36) in this setting.

Therefore consider an easy set up without varying noise nor a complex mask. To ensure a certain definition, we choose the signal space to be a one dimensional regular grid with 2048 lattice points in one dimension. The synthetic signal and corresponding synthetic data are drawn from the prior specified in section 3.1. The data is masked, such that only the central 256 pixels are measured. Those data are then compressed to four data points, from which the signal is inferred in a last step.

Besides, the synthetic signal and data are computed as before. However, the noise standard deviation now is constantly $0.2 \cdot 10^{-2}$ and the response is set to be a mask measuring pixels 896 to 1152 leading to a transparent window of 256 pixels in the center of the grid. The measurement setup with signal mean, synthetic signal and data can be seen in Figure 13.

The consequential mean and uncertainty for the inference with the original data and the ones with the compressed data are plotted together with the ground truth in figure 14. The original data has been compressed from 256 to 4 data points.

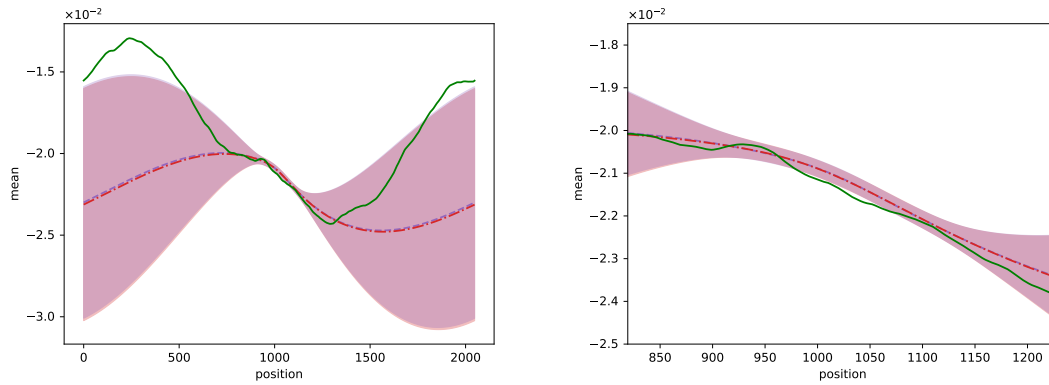


Figure 14: The same as Figure 2 but for the setup shown in Figure 13.

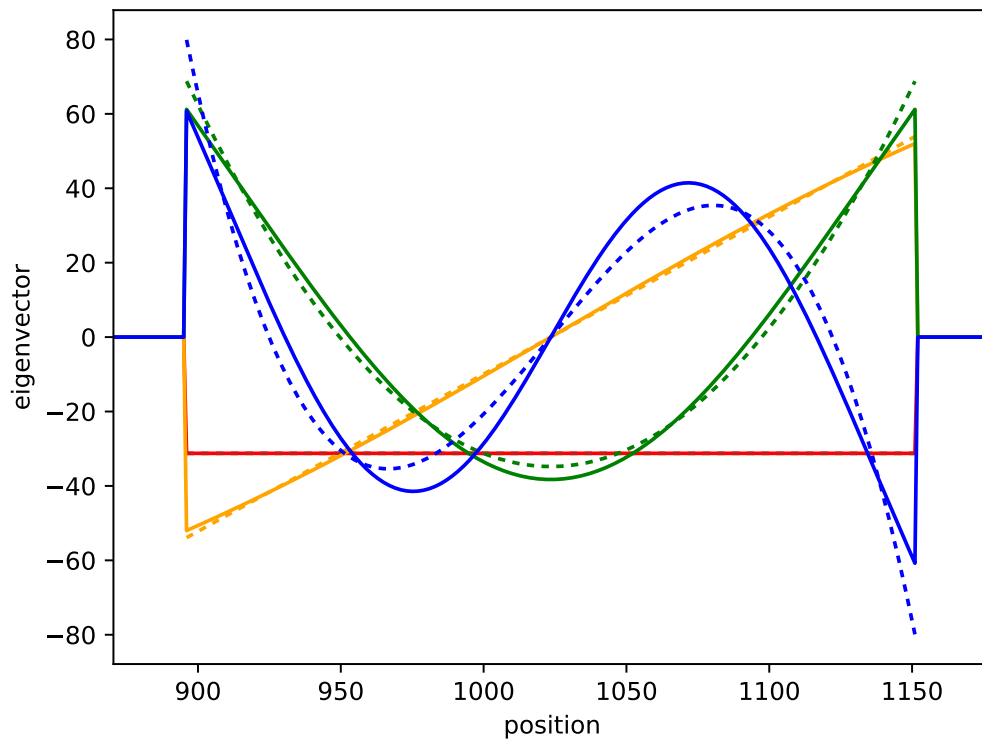


Figure 15: The first four eigenvectors (solid lines) as in Figure 3 but for the setup shown in Figure 13 together with the first four Chebyshev polynomials (dashed lines).

Now let us have a closer look at the eigenvectors plotted in Figure 15, which correspond to a back projection with R_c of the corresponding single data point being one and all the others being zero. These functions remind of Chebyshev polynomials of the first kind. Those were fitted to the eigenvectors minimizing the mean squared error and are plotted in the same figure as the eigenvectors. One can clearly see their similarity. The lower order polynomials fit the best, while higher order polynomials deviate especially at the edges.

An analytical analysis is done in the next section.

7 Analytical solution of the 1D Wiener Filter Data Compression

In this section we will derive the eigenfunctions of (36) analytically for some signal on a one dimensional line covered by a mask of length L starting at $x = 0$. The response of the linear measurement equation is

$$R_{\mathbf{o}xx'} = \delta(x - x')\chi_{[0,L]}(x'), \text{ with} \quad (71)$$

$$\chi_{[0,L]}(x) := \begin{cases} 1 & \text{for } x \in [0, L] \\ 0 & \text{else} \end{cases}. \quad (72)$$

The Gaussian noise n in the measured area has the covariance

$$N_{\mathbf{o}xx'} = n_{\text{const}}\delta(x - x'). \quad (73)$$

Having a look on the eigenvalue problem (36)

$$M_{\mathbf{o}}Sr_i = \mu_i^2r_i \quad (74)$$

with

$$M_{\mathbf{o}} = R_{\mathbf{o}}^\dagger N_{\mathbf{o}} R_{\mathbf{o}}, \quad (75)$$

we see, that $r_i(x) = 0$ for $x \notin [0, L]$ and $\mu_i \neq 0$. For $x \in [0, L]$

$$Sr_i = \frac{\mu_i^2}{n_{\text{const}}}r_i =: \lambda_i r_i. \quad (76)$$

We specified S by a falling power spectrum following a power law with spectral index of -2α in Hartley space.

$$S = \mathbb{H}P(|k|)\mathbb{H}^\dagger \quad (77)$$

$$= \left(\mathbb{H} \frac{1}{k^\alpha} \right)^{1+\dagger} = (\Delta^{-\frac{\alpha}{2}})^\dagger \Delta^{-\frac{\alpha}{2}} \quad (78)$$

with Hartley transform

$$\mathbb{H}_{xk} = \frac{1}{\sqrt{2\pi}} \int dk [\cos(kx) + \sin(kx)] \quad (79)$$

and Laplace operator

$$\Delta = \nabla^2 = \sum_i \partial_{x_i}^2. \quad (80)$$

Then

$$\lambda_i r_i = S r_i = \Delta^{-\alpha} r_i = \lambda_{\Delta_i}^{-\alpha} r_i \quad (81)$$

with eigenfunction r_i and eigenvalue λ_{Δ_i} of the Laplace operator. This is equivalent to the Helmholtz equation with opposite sign. Its eigenfunctions in 2D are the Bessel functions. In one dimension with $\alpha = 2$ as in section 3.1, the covariance operator becomes $S = \partial_x^{-4}$, thus

$$\partial_x^{-4} r_i = \lambda_{\Delta_i}^{-2} r_i. \quad (82)$$

The square of the eigenvalue ensures the eigenvalues of the prior covariance to be positive. Since $\lambda_i = \lambda_{\Delta_i}^{-\alpha}$, λ_i does not become zero.

The solution to this problem are super positions of exponential functions of the same eigenvalue

$$r_i(x) = a e^{+\sqrt{\lambda_i} x} + b e^{-\sqrt{\lambda_i} x}, \quad (83)$$

such as $\cosh(\sqrt{\lambda_i} x)$ and $\sinh(\sqrt{\lambda_i} x)$ for positive λ_i , as well as $\cos(\sqrt{-\lambda_i} x)$ and $\sin(\sqrt{-\lambda_i} x)$ for negative λ_i . For eigenvalue $\lambda_{\Delta_i} = 0$, also polynomials up to third order are eigenfunctions to the Laplace operator. Those belong to the largest eigenvalues of S , which are also the most informative ones according to Equation (33). This explains the proximity of the eigenmodes to Chebyshev polynomials as observed in Figure 15 for a signal power spectrum that asymptotically follows k^{-4} .